

LETTERS

The menthol receptor TRPM8 is the principal detector of environmental cold

Diana M. Bautista^{1,2*}, Jan Siemens^{1,2*}, Joshua M. Glazer^{5*}, Pamela R. Tsuruda^{1,2}, Allan I. Basbaum^{3,4}, Cheryl L. Stucky⁵, Sven-Eric Jordt⁶ & David Julius^{1,2}

Sensory nerve fibres can detect changes in temperature over a remarkably wide range, a process that has been proposed to involve direct activation of thermosensitive excitatory transient receptor potential (TRP) ion channels^{1–4}. One such channel—TRP melastatin 8 (TRPM8) or cold and menthol receptor 1 (CMR1)—is activated by chemical cooling agents (such as menthol) or when ambient temperatures drop below ~26 °C, suggesting that it mediates the detection of cold thermal stimuli by primary afferent sensory neurons^{5,6}. However, some studies have questioned the contribution of TRPM8 to cold detection or proposed that other excitatory or inhibitory channels are more critical to this sensory modality *in vivo*^{7–10}. Here we show that cultured sensory neurons and intact sensory nerve fibres from TRPM8-deficient mice exhibit profoundly diminished responses to cold. These animals also show clear behavioural deficits in their ability to discriminate between cold and warm surfaces, or to respond to evaporative cooling. At the same time, TRPM8 mutant mice are not completely insensitive to cold as they avoid contact with surfaces below 10 °C, albeit with reduced efficiency. Thus, our findings demonstrate an essential and predominant role for TRPM8 in thermosensation over a wide range of cold temperatures, validating the hypothesis² that TRP channels are the principal sensors of thermal stimuli in the peripheral nervous system.

We generated TRPM8-deficient mice through targeted deletion of a genomic region encoding amino acids 594–661 within the presumptive cytoplasmic amino-terminal domain. In addition to removing coding information, this manipulation introduced a stop codon before and a frameshift after the deleted segment (Fig. 1a). Successful targeting was verified by Southern blotting and RT-PCR analysis of transcripts from trigeminal ganglia of wild-type and mutant mice (Fig. 1b). The resulting *TRPM8*^{-/-} mice were normal in overall appearance and viability, and matings between heterozygous animals produced siblings with normal mendelian distributions for gender and genotype. Moreover, mutant and wild-type littermates showed no differences in core body temperature (37.4 ± 0.15 °C and 37.4 ± 0.13 °C, respectively; *n* = 11 mice per genotype).

Sensory ganglia from TRPM8-deficient mice appeared anatomically normal, as was assessed by staining with a variety of immunological probes that label peptidergic, unmyelinated or vanilloid-responsive neurons (Fig. 1c, d). Thus, antibodies directed against substance P (peripherin) or the capsaicin receptor (TRPV1) revealed an identical prevalence of labelled cells in trigeminal ganglia from wild-type and mutant mice. In contrast, TRPM8 immunoreactivity was specifically absent from trigeminal ganglia or the peripheral free nerve endings of adult mutant mice. Central projections of primary afferent fibres to the spinal cord of *TRPM8*^{-/-} mice were also devoid of TRPM8

immunoreactivity, while those from wild-type littermates showed a robust pattern of staining that was confined to the most superficial layer of the dorsal horn (lamina I), a region that is innervated by primary afferent nociceptors, including those expressing TRPV1. Importantly, polymerase chain reaction (PCR) analysis showed that *TRPM8*^{-/-} mice produce a truncated non-functional transcript from the disrupted locus, enabling us to demonstrate by *in situ* hybridization histochemistry that loss of TRPM8 protein expression does not eliminate neurons that normally express this channel (Supplementary Fig. 1).

Functional disruption of the *TRPM8* gene was assessed by using live-cell calcium imaging to measure the sensitivity of trigeminal and dorsal root ganglion neurons to cooling agents. Consistent with previous observations^{5,11}, approximately 17% of neurons cultured from wild-type ganglia showed rapid and robust responses to bath applied menthol (100 μM) or the super-cooling agent icilin (100 μM). Neurons from *TRPM8*^{-/-} mice were completely unresponsive to either compound (Fig. 2a, b). In contrast, TRPM8-deficient neurons displayed normal sensitivity to capsaicin or the TRPA1 agonist, allyl isothiocyanate (mustard oil)^{12,13} (Fig. 2b). Icilin, which is a weak TRPA1 agonist¹⁴, activated all mustard-oil-sensitive neurons at concentrations over 500 μM, regardless of genotype (not shown). Together, these results verify selective loss of TRPM8 activity in mutant mice and suggest that this channel is the sole target through which menthol and icilin mediate their cooling effects.

Next, we asked whether TRPM8 ablation affects cellular cold sensitivity. When challenged with a cooling gradient (30 to 8 °C over 30 s), ~22% of trigeminal neurons from wild-type mice showed significant increases in cellular calcium levels, as previously described¹¹ (Fig. 2c, d). These cold-sensitive neurons could be segregated into two distinct populations: most (77%) were menthol-sensitive, showed a rapid activation rate ($dCa^{2+}/dT = 40 \text{ nmol s}^{-1}$), and had an average response threshold of 22 °C when cooled from a holding temperature of 30 °C. As observed with the cloned TRPM8 channel, the activation threshold of this neuronal subpopulation shifted to 16 °C when cooled from a holding temperature of 22 °C (not shown), suggesting that both cloned and native channels show adaptation¹⁵. The remaining 23% of cold-sensitive neurons (5% of all neurons) were menthol-, capsaicin- and mustard-oil-insensitive; they showed a substantially slower cold activation rate ($dCa^{2+}/dT = 4 \text{ nmol s}^{-1}$), smaller peak cold-evoked calcium response (300 nM), and had an average response threshold of 12 °C irrespective of starting temperature. Trigeminal neurons from *TRPM8*^{-/-} mice showed a dramatic reduction in the total number of cold-sensitive neurons, with only 4% of cells responding to the cold ramp (Fig. 2c, d). The response properties of these residual cold-sensitive neurons closely matched those of the

¹Department of Physiology, ²Department of Cellular and Molecular Pharmacology, ³Departments of Anatomy and Physiology, ⁴W. M. Keck Center for Integrative Neuroscience, University of California, San Francisco, California 94143, USA. ⁵Department of Cell Biology, Neurobiology and Anatomy, Medical College of Wisconsin, Milwaukee, Wisconsin 53226, USA. ⁶Department of Pharmacology, Yale University School of Medicine, New Haven, Connecticut 06520, USA.

*These authors contributed equally to this work.

menthol-insensitive population present in cultures from wild-type ganglia. Thus *TRPM8* ablation results in a profound reduction in both the number and magnitude of cellular cold responses, leaving intact a small cohort of neurons that respond to cold with an activation threshold of $\sim 12^\circ\text{C}$, and probably correspond to the menthol-insensitive component of cold-sensitive neurons from wild-type ganglia. No significant differences in chemical or thermal responses were observed between dorsal root ganglia and trigeminal neurons, irrespective of genotype (Supplementary Table 1).

In contrast to differences in cold sensitivity, *TRPM8*-deficient neurons showed normal responses to heat. When exposed to a heat ramp (30 to 45°C in 45 s), 44% of trigeminal neurons from *TRPM8*^{-/-} mice were heat-sensitive, compared with 41% from wild-type littermates. Conversely, mice lacking the capsaicin receptor TRPV1 showed a normal prevalence of cold-sensitive neurons, but a substantial reduction in the number of cells responding to heat, as expected (Fig. 2d).

We next used the skin-nerve preparation to ask whether *TRPM8* mediates cold responses at the peripheral terminals of cutaneous afferent fibres^{16,17}. When subjected to a cold ramp (32 to 2°C over 20 s), 35% of C fibres from wild-type mice showed robust action potential firing. As expected, cold-evoked firing rates of these fibres showed adaptation within the first 8 s of the cold ramp (Supplementary Fig. 2b). In contrast, only 5.4% of C fibres from

TRPM8-deficient mice responded to cold ($P < 0.0001$; Fisher's exact test; Fig. 3a, b), and these residual cold-sensitive units had significantly decreased firing rates (Fig. 3b; $P < 0.0001$; *t*-test). Basal (ongoing) action potential firing at skin temperature (32°C) is a property of cold-sensitive fibres^{18,19}, and indeed we found that wild-type cold-activated C fibres had significantly higher baseline firing rates than cold-insensitive fibres (Supplementary Fig. 2a). The number of C fibres showing baseline activity did not differ significantly when comparing wild-type and *TRPM8*-deficient preparations (60% versus 45%; $P = 0.14$, Fisher's exact test). However, C fibres from *TRPM8*-deficient mice showed a significantly reduced basal firing rate, akin to that observed in cold-insensitive units from wild-type littermates (Supplementary Fig. 2a). These results suggest that *TRPM8* also modulates the characteristic basal firing rate of the majority of cold-sensitive C fibres. Among myelinated A δ fibres, cold also elicited firing of A-mechanoreceptors (AM), albeit less robustly than generally observed with unmyelinated C fibres (Fig. 3c). In wild-type preparations, 16.7% of these units showed cold-evoked action potentials, whereas only 1 of 26 (3.9%) AM fibres from *TRPM8*-deficient mice responded with comparable firing rates (Fig. 3d).

In contrast to these robust deficits in cold sensitivity, the electrical response characteristics of *TRPM8*-deficient fibres, including conduction velocity and electrical activation threshold, were almost identical to those of wild-type littermates. Furthermore, the

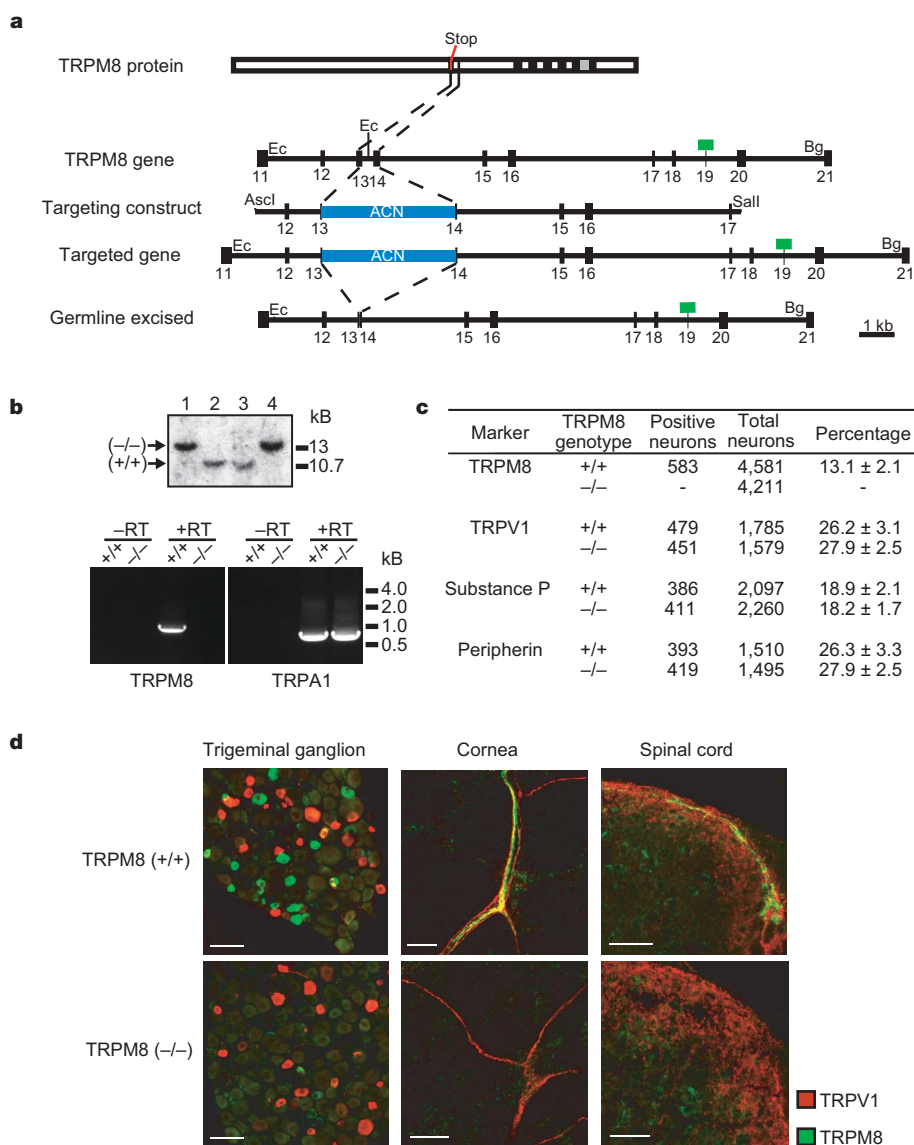


Figure 1 | Generation and histological analysis of *TRPM8*-deficient mice. **a**, *TRPM8* gene targeting strategy introduces a stop codon within the protein-coding region. Transmembrane and pore loop domains are indicated by black and grey bars, respectively; exons are numbered (black bars on genomic map); blue bar depicts self-excising ACN neomycin expression cassette; green bar denotes 3' probe. Restriction sites indicated are *EcoRI* (Ec), *BglI* (Bg), *SallI* and *AsclI*. **b**, Southern blot (top) confirms targeting of *TRPM8* locus, where *BglI* and *EcoRI* digests produce expected fragments of 13 and 10.7 kilobases (kb) for wild-type and mutant alleles, respectively. RT-PCR (bottom) confirms the absence of normal *TRPM8* transcripts in trigeminal ganglia from *TRPM8*^{-/-} mice. Primers amplifying a 1 kb region from exon 13 of the *TRPM8* gene do not generate a product with RNA from *TRPM8*^{-/-} ganglia. As positive control, a 700 base pair (bp) region of *TRPA1* was amplified from wild-type or *TRPM8*^{-/-} ganglia. **c**, Immunohistochemical analysis using anti-TRPV1, anti-substance P, or anti-peripherin antibodies shows similar distribution of labelled cells in *TRPM8*-deficient and wild-type trigeminal ganglia. In contrast, *TRPM8* immunoreactivity is absent from *TRPM8*^{-/-} ganglia, whereas wild-type sections show staining in $\sim 13\%$ of neurons (2–3 animals per genotype). Percentages represent mean \pm s.e.m. **d**, Immunostaining of trigeminal ganglia (left), corneal afferents (middle), and spinal cord dorsal horn (right) with anti-TRPM8 (green) and anti-TRPV1 (red) antibodies reveals selective loss of *TRPM8* expression in *TRPM8*^{-/-} mice. Scale bars, 50 μm .

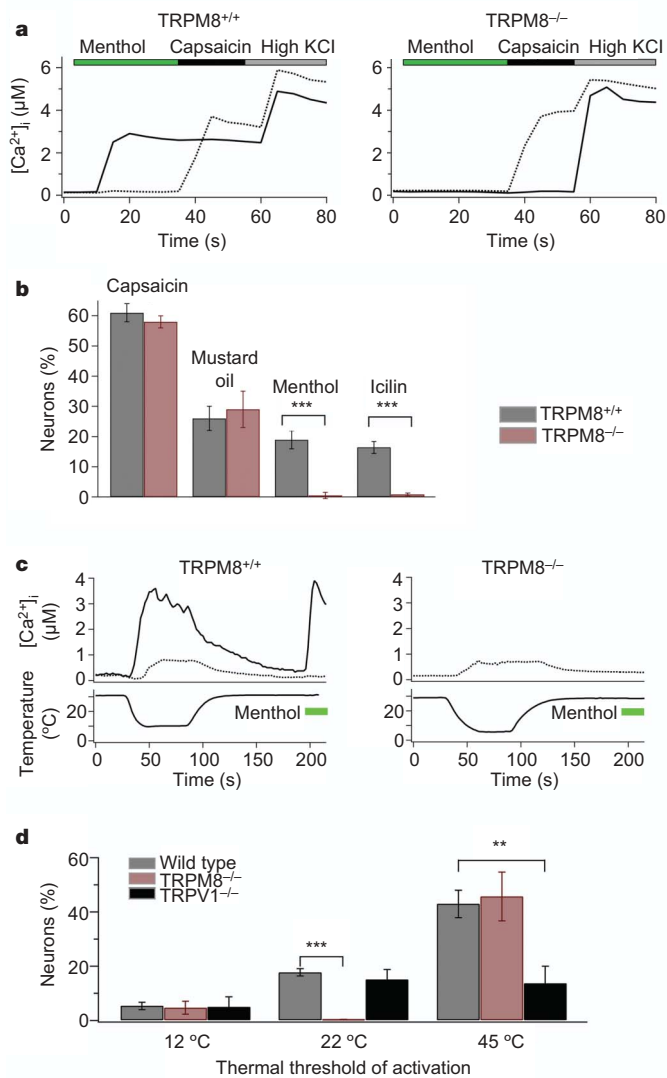


Figure 2 | TRPM8-deficient neurons show loss of menthol and cold sensitivity. **a**, Trigeminal neurons from *TRPM8*^{+/+} (left) or *TRPM8*^{-/-} (right) mice were challenged with menthol (100 μ M), followed by capsaicin (1 μ M), then high KCl (75 mM). Responses were assessed by calcium imaging. *TRPM8*^{+/+} ganglia displayed two distinct subpopulations: menthol-sensitive (solid trace) and capsaicin-sensitive (dotted trace) neurons. No menthol sensitivity was detected in *TRPM8*^{-/-} neurons ($n = 50$ cells per trace). Similar results were obtained with 50 or 250 μ M menthol (not shown). **b**, Prevalence of sensory neurons responding to capsaicin (1 μ M), allyl isothiocyanate (mustard oil, 100 μ M), menthol (100 μ M) or icilin (100 μ M) from *TRPM8*^{+/+} and *TRPM8*^{-/-} ganglia. **c**, Trigeminal neurons were challenged with cold and menthol (green bar) and responses assessed by calcium imaging. In wild-type ganglia, menthol-sensitive neurons (solid trace) showed robust cold responses (threshold 22 \pm 1.5 $^{\circ}$ C), and some menthol-insensitive neurons (dotted trace) showed low-level responses (threshold 12 \pm 1.5 $^{\circ}$ C). *TRPM8*^{-/-} ganglia contained few cold responders, which resembled the latter population. No significant differences were observed between dorsal root ganglia and trigeminal neurons, irrespective of genotype (Supplementary Table 1). **d**, Comparison of cold and heat sensitivity for wild type, *TRPM8*^{-/-} and *TRPV1*^{-/-} neurons. For wild-type ganglia (grey bars) 4% of neurons were activated with a threshold of 12 $^{\circ}$ C, 17% at 22 $^{\circ}$ C, and 44% at 45 $^{\circ}$ C. The 22 $^{\circ}$ C threshold group was absent from *TRPM8*^{-/-} ganglia (red bars), while the 12 $^{\circ}$ C and 45 $^{\circ}$ C populations were unaltered. In contrast, the 45 $^{\circ}$ C population was substantially reduced (to 14%) in *TRPV1*^{-/-} ganglia (black bars), whereas cold-sensitive populations were unaltered ($n > 420$ neurons per genotype). ** $P < 0.01$, *** $P < 0.001$, one-way analysis of variance (ANOVA) analysis followed by Tukey's HSD post-hoc analysis. No significant differences were observed when comparing chemical or thermal sensitivity of wild-type and *TRPM8* heterozygous neurons (not shown). Graphs display mean \pm s.e.m.

mechanical thresholds of C and AM fibres did not differ significantly between genotypes (Supplementary Fig. 2d). Taken together, these findings demonstrate that loss of TRPM8 expression results in a selective deficit in cold sensitivity of both C and AM fibres, without affecting other aspects of electrical and mechanical excitability.

To assess behavioural cold sensitivity, we first measured acute finching responses to acetone-evoked evaporative cooling of the hind paw. *TRPM8*-deficient mice showed a significant reduction (~50%) in this nocifensive response compared to wild-type littermates (Fig. 4a). Next, we asked whether these animals also exhibit deficits in their ability to discriminate between warm and cold

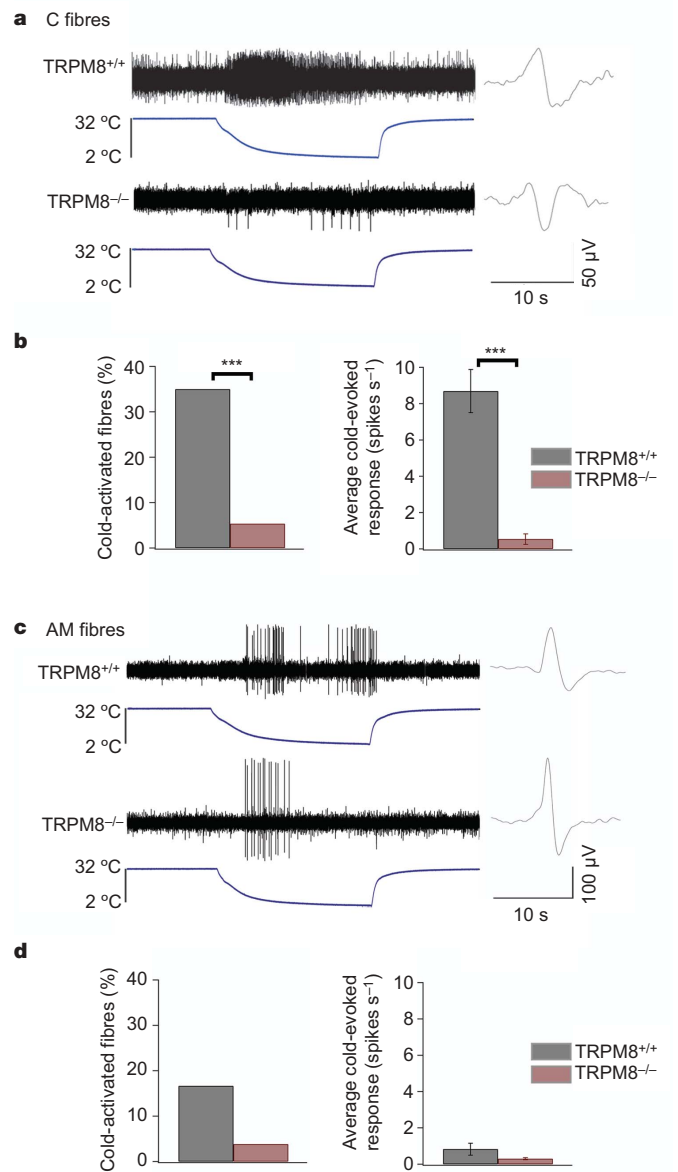


Figure 3 | TRPM8-deficient nerve fibres show loss of cold sensitivity. **a**, Typical response of wild-type (top) and *TRPM8*-deficient (bottom) cutaneous C fibre to a cold ramp (32 to 2 $^{\circ}$ C, over 20 s). Action potential waveform is shown to right of trace. **b**, Percentage of C fibres responding to cold ramp in wild-type (black; $n = 60$) versus *TRPM8*^{-/-} (red; $n = 56$) mice (left). Average cold-evoked action potential firing rate in C fibres of wild-type ($n = 21$) versus *TRPM8*^{-/-} ($n = 3$) mice (right; mean \pm s.e.m.). **c**, Typical response of wild-type (top) and *TRPM8*-deficient (bottom) cutaneous AM fibre to a cold ramp (32 to 2 $^{\circ}$ C, over 20 s). **d**, Percentage of AM fibres responding to cold ramp in wild-type (black; $n = 24$) versus *TRPM8*^{-/-} (red; $n = 26$) mice (left). Average cold-evoked action potential firing rate in AM fibres of wild-type ($n = 4$; mean \pm s.e.m.) versus *TRPM8*^{-/-} ($n = 1$) mice (right). *** $P < 0.001$, Student's *t*-test or Fisher's exact test.

surfaces. Animals were allowed to explore adjacent surfaces, with one held at 30 °C and the other ranging from 49 to 5 °C (Fig. 4b). The percentage of time spent on the 30 °C surface was measured over a 5 min period. When placed on equivalent temperatures (both 30 °C), neither wild-type nor mutant mice displayed a preference, spending equal time on each side, as expected (Fig. 4c). As the variable plate was cooled, wild-type mice showed a clear preference for the 30 °C side, spending less time on the cold side as temperature decreased. In striking contrast, TRPM8-deficient littermates showed relatively little, if any, preference for the 30 °C side until the adjacent surface dropped below 15 °C (Fig. 4c), a threshold that has been suggested to represent a demarcation between innocuous cool and noxious cold in primates²⁰. But even at these lower temperatures, TRPM8^{-/-} mice explored the cold surface for an extended period, taking substantially more time than wild-type littermates to appreciate the aversive nature of the environment relative to the warmer side. Wild-type and mutant mice also exhibited striking differences in their patterns of

exploratory behaviour when approaching a cold surface. After their initial contact with the colder surface, wild-type animals approached the plate with apparent trepidation, making only rapid and brief contact with their front paws before withdrawing to the warmer side. In contrast, TRPM8-deficient mice made full transitions to the cold side and showed relatively uninhibited exploratory behaviour, as reflected by the greater number of crossings between adjacent surfaces (Supplementary Video 1). Nonetheless, mutant mice displayed normal preference for 30 °C over noxious heat (49 °C), and thus did not exhibit a general deficiency in thermosensation (Fig. 4c).

We also examined nocifensive behaviours by placing animals on a single plate set to a variety of noxious temperatures. Equivalent licking, flinching or shivering responses were observed when TRPM8-deficient or wild-type mice were placed on a plate set to 52, 10, 0 or -5 °C (Fig. 4d). No behavioural responses were observed at non-noxious settings of 20 and 30 °C (not shown). Similar findings were obtained using a behavioural paradigm that measures time to paw withdrawal from a radiant heat source, where mutant and wild-type mice showed similar latencies (11.8 ± 0.42 s and 12.2 ± 0.49 s, respectively; *n* = 11 per genotype; Supplementary Fig. 3). Baseline mechanical sensitivity was also normal in TRPM8-deficient mice; paw-withdrawal thresholds to graded mechanical force did not differ with genotype (0.77 ± 0.12 g and 0.73 ± 0.09 g for TRPM8^{-/-} and TRPM8^{+/+} littermates, respectively; *n* = 23 per genotype; Supplementary Fig. 3). Taken together, our results show that TRPM8 is specifically required for normal cold sensation, but not for the detection of pressure or heat.

Cloning of the capsaicin receptor TRPV1 and its heat-sensitive homologue TRPV2 led to the prediction that a family of TRP channel subtypes mediates peripheral temperature detection over a wide physiological range, from hot to cold². Molecular characterization of TRPM8 bolstered this hypothesis because the electrophysiological and pharmacological properties of the cloned channel resemble those of a major subclass of native cold-evoked membrane currents^{5,10,15,21}. However, some studies have suggested that a significant component of cold-evoked neuronal depolarization or fibre excitation is mediated by other entities, such as epithelial sodium channels, TRPA1, background potassium channels, or ion pumps^{7,8,14,22–24}. It has also been proposed that cold evokes psychophysical sensations through its effects on vascular tone, which are then transduced to sensory afferents indirectly^{25,26}. Our present results show that TRPM8 is essential for a large component of cold sensitivity, whether assessed at the cellular, nerve terminal or behavioural level. These findings solidify the importance of this channel, and the primary afferent nerve fibre, for the direct detection of environmental cold. More generally, our results confirm the hypothesis that TRP channels serve as the principal transducers of thermal stimuli within the mammalian peripheral nervous system.

TRPM8-deficient mice retain a small, but finite number of cold-sensitive neurons, consistent with our fibre recordings showing a small residual population of cold-sensitive C and AM units. Moreover, these animals display aversion to cold at temperatures below 15 °C, which is considered to be an approximate demarcation between innocuous cool and noxious cold^{20,27}. These observations suggest that TRPM8-independent mechanisms exist for the detection of cold, and are consistent with a number of cellular studies describing a population of menthol-insensitive, cold-sensitive neurons^{11,14,28}. The residual cold-sensitive neurons and fibres that we observe in TRPM8-deficient mice probably correspond to this population on the basis of the similar prevalence and activation threshold of ~12 °C. The molecular mechanism underlying this small, but finite cold sensitivity remains unknown, but could involve modulation of other excitatory or inhibitory channels on primary afferent sensory neurons. The mustard-oil receptor TRPA1 has been proposed to function as a detector of noxious cold by menthol-insensitive nociceptors¹⁴, although recent electrophysiological and genetic studies suggest otherwise^{11,15,29,30}. In any case, our present

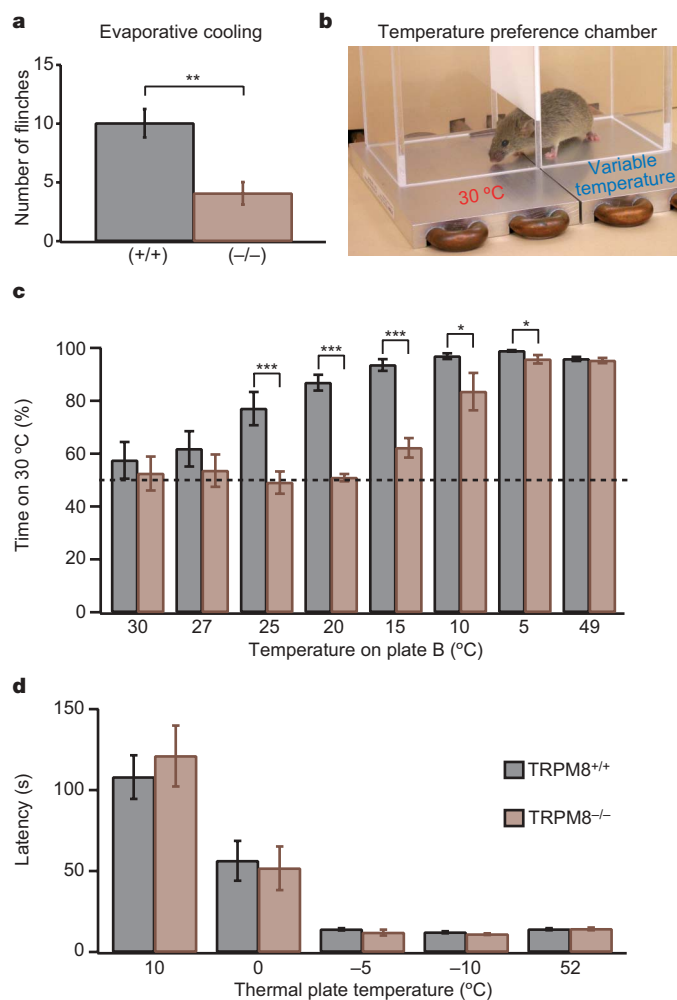


Figure 4 | TRPM8 is required for normal cold-evoked behaviours.

a, Licking and flinching in response to evaporative cooling was measured for 1 min following application of acetone (50 μ l) to the hind paw. TRPM8^{-/-} mice displayed significantly decreased behaviour compared to TRPM8^{+/+} littermates (*n* = 21 mice per genotype). **b**, Mouse in temperature preference chamber. **c**, TRPM8^{+/+} and TRPM8^{-/-} littermates were allowed to choose between adjacent surfaces adjusted to 30 °C versus a range of temperatures, as shown. The percentage of time spent at 30 °C over a 5 min period is shown (*n* \geq 10 mice per genotype). **d**, Latency to licking or flinching of the hind paw was measured following placement of mice on a single platform set to a variety of temperatures, as shown. TRPM8^{+/+} and TRPM8^{-/-} littermates displayed similar latencies at all temperatures examined (*n* = 6 mice per genotype). **P* < 0.05, ***P* < 0.01, ****P* < 0.001, one-way ANOVA with Tukey's HSD post-hoc analysis. Graphs display mean \pm s.e.m.

results show that the residual cold-sensitive neurons in TRPM8-deficient mice are not mustard-oil-sensitive, suggesting that TRPA1 does not underlie this response. Consistent with these cellular findings, TRPA1-deficient mice (males or females) were indistinguishable from wild-type littermates when examined for behavioural responses to cold using the two-plate choice test (Supplementary Fig. 4). Furthermore, a recent analysis of skin-nerve preparations from TRPA1-deficient mice showed no deficit in cold responsiveness in either C or A fibre nociceptors (C.L.S. and personal communication from K. Y. Kwan).

Our behavioural analysis shows that TRPM8 constitutes the primary, if not sole determinant of thermosensitivity in the cool range, and that it also contributes to the detection of noxious cold, defined as temperatures below 15 °C. It remains to be determined whether the small residual population of cold-sensitive neurons and fibres enables TRPM8^{-/-} mice to recognize noxious cold. In addition to activating TRPM8, noxious cold may also activate sensory nerve fibres indirectly by provoking tissue injury or changes in vascular tone, thereby leading to the production or release of pro-algesic agents that evoke pain by stimulating nociceptors. Alternatively, aversion to noxious cold may be triggered by the inhibition of warm-sensing fibres. TRPM8-deficient mice now provide a genetic model with which to dissect this residual aspect of cold sensation.

METHODS

Mouse genetics. TRPM8-deficient mice were generated through homologous recombination in E14Tg2A.4 embryonic stem cells. Positive clones were injected into C57/Bl6 blastocysts and male chimaeras mated to C57/Bl6 females. Heterozygotes thus produced were crossed to generate paired F2 littermates for all studies.

Histology. Frozen paraformaldehyde-fixed tissue sections were prepared from trigeminal ganglia of wild-type or TRPM8-deficient mice and incubated with a variety of previously characterized antibody or nucleic acid probes. For any given marker, quantification of labelled cells was assessed while blind to genotype.

Cell and nerve fibre physiology. Dissociated sensory neurons from trigeminal or dorsal root ganglia of wild-type and TRPM8-deficient mice were placed in culture and analysed for chemical or thermal sensitivity using Fura 2-AM based ratiometric calcium imaging. The skin-nerve preparation was used to obtain electrophysiological recordings from desheathed saphenous nerve. Single afferent units were identified using an unbiased electrical search stimulus and subsequently examined for responsiveness to a cold ramp in which perfusate temperature decreased from 32 to 2 °C over 20 s. Both calcium imaging and nerve fibre recording were carried out with preparations from individual littermates while blind to genotype.

Behaviour. Cold sensitivity was assessed using acetone-evoked evaporative cooling or two-plate choice tests. Response latencies to noxious temperatures were measured using radiant heating or single hot/cold plate paradigms. Mechanical thresholds were determined using calibrated von Frey filaments. Behavioural studies were carried out with paired littermates while blind to genotype. All experiments were performed according to the policies and recommendations of the International Association for the Study of Pain and approved by the University of California, San Francisco Institution Animal Care and Use Committee.

Full Methods and any associated references are available in the online version of the paper at www.nature.com/nature.

Received 22 March; accepted 14 May 2007.

Published online 30 May 2007.

- Jordt, S. E., McKemy, D. D. & Julius, D. Lessons from peppers and peppermint: the molecular logic of thermosensation. *Curr. Opin. Neurobiol.* **13**, 487–492 (2003).
- Caterina, M. J., Rosen, T. A., Tominaga, M., Brake, A. J. & Julius, D. A capsaicin-receptor homologue with a high threshold for noxious heat. *Nature* **398**, 436–441 (1999).
- Dhaka, A., Viswanath, V. & Patapoutian, A. Trp ion channels and temperature sensation. *Annu. Rev. Neurosci.* **29**, 135–161 (2006).
- Lumpkin, E. A. & Caterina, M. J. Mechanisms of sensory transduction in the skin. *Nature* **445**, 858–865 (2007).
- McKemy, D. D., Neuhauser, W. M. & Julius, D. Identification of a cold receptor reveals a general role for TRP channels in thermosensation. *Nature* **416**, 52–58 (2002).
- Peier, A. M. *et al.* A TRP channel that senses cold stimuli and menthol. *Cell* **108**, 705–715 (2002).
- Viana, F., de la Pena, E. & Belmonte, C. Specificity of cold thermotransduction is determined by differential ionic channel expression. *Nature Neurosci.* **5**, 254–260 (2002).
- Madrid, R. *et al.* Contribution of TRPM8 channels to cold transduction in primary sensory neurons and peripheral nerve terminals. *J. Neurosci.* **26**, 12512–12525 (2006).
- Reid, G. & Flonta, M. Cold transduction by inhibition of a background potassium conductance in rat primary sensory neurones. *Neurosci. Lett.* **297**, 171–174 (2001).
- McKemy, D. D. How cold is it? TRPM8 and TRPA1 in the molecular logic of cold sensation. *Mol. Pain* **1**, 16–22 (2005).
- Bautista, D. M. *et al.* TRPA1 mediates the inflammatory actions of environmental irritants and proalgesic agents. *Cell* **124**, 1269–1282 (2006).
- Bandell, M. *et al.* Noxious cold ion channel TRPA1 is activated by pungent compounds and bradykinin. *Neuron* **41**, 849–857 (2004).
- Jordt, S. E. *et al.* Mustard oils and cannabinoids excite sensory nerve fibres through the TRP channel ANKTM1. *Nature* **427**, 260–265 (2004).
- Story, G. M. *et al.* ANKTM1, a TRP-like channel expressed in nociceptive neurons, is activated by cold temperatures. *Cell* **112**, 819–829 (2003).
- Reid, G. ThermoTRP channels and cold sensing: what are they really up to? *Pflugers Arch.* **451**, 250–263 (2005).
- Stucky, C. L. *et al.* Overexpression of nerve growth factor in skin selectively affects the survival and functional properties of nociceptors. *J. Neurosci.* **19**, 8509–8516 (1999).
- Koltzenburg, M., Stucky, C. L. & Lewin, G. R. Receptive properties of mouse sensory neurons innervating hairy skin. *J. Neurophysiol.* **78**, 1841–1850 (1997).
- Iggo, A. Cutaneous thermoreceptors in primates and sub-primates. *J. Physiol. Lond.* **200**, 403–430 (1969).
- Schafer, K., Braun, H. A. & Kurten, L. Analysis of cold and warm receptor activity in vampire bats and mice. *Pflugers Arch.* **412**, 188–194 (1988).
- Rainville, P., Chen, C. C. & Bushnell, M. C. Psychophysical study of noxious and innocuous cold discrimination in monkey. *Exp. Brain Res.* **125**, 28–34 (1999).
- Reid, G. & Flonta, M. L. Cold current in thermoreceptive neurons. *Nature* **413**, 480 (2001).
- Maingret, F. *et al.* TREK-1 is a heat-activated background K(+) channel. *EMBO J.* **19**, 2483–2491 (2000).
- Askwith, C. C., Benson, C. J., Welsh, M. J. & Snyder, P. M. DEG/ENaC ion channels involved in sensory transduction are modulated by cold temperature. *Proc. Natl Acad. Sci. USA* **98**, 6459–6463 (2001).
- Pierau, F. K., Torrey, P. & Carpenter, D. O. Mammalian cold receptor afferents: role of an electrogenic sodium pump in sensory transduction. *Brain Res.* **73**, 156–160 (1974).
- Kreh, A., Anton, F., Gilly, H. & Handwerker, H. O. Vascular reactions correlated with pain due to cold. *Exp. Neurol.* **85**, 533–546 (1984).
- Fruhstorfer, H. & Lindblom, U. Vascular participation in deep cold pain. *Pain* **17**, 235–241 (1983).
- Hensel, H. & Zotterman, Y. The effect of menthol on the thermoreceptors. *Acta Physiol. Scand.* **24**, 27–34 (1951).
- Babes, A., Zorzon, D. & Reid, G. A novel type of cold-sensitive neuron in rat dorsal root ganglia with rapid adaptation to cooling stimuli. *Eur. J. Neurosci.* **24**, 691–698 (2006).
- Zurborg, S., Yurgionas, B., Jira, J. A., Caspani, O. & Heppenstall, P. A. Direct activation of the ion channel TRPA1 by Ca(2+). *Nature Neurosci.* **10**, 277–279 (2007).
- Doerner, J. F., Gisselmann, G., Hatt, H. & Wetzel, C. H. Transient receptor potential channel A1 is directly gated by calcium ions. *J. Biol. Chem.* (2007).

Supplementary Information is linked to the online version of the paper at www.nature.com/nature.

Acknowledgements We thank R. Nicoll for discussion and criticism, M. Tominaga for providing TRPM8 antiserum, T. Nikai for advice regarding behavioural assays, and J. Poblete for technical assistance throughout. This work was supported by grants from the NIH (D.J., A.I.B., S.-E.J. and C.L.S.), a Burroughs Wellcome Fund Career Award in Biomedical Sciences (D.M.B.) and a postdoctoral fellowship from the International Human Frontier Science Program Organization (J.S.).

Author Information Reprints and permissions information is available at www.nature.com/reprints. The authors declare no competing financial interests. Correspondence and requests for materials should be addressed to D.J. (julius@cmp.ucsf.edu), S.-E.J. (sven.jordt@yale.edu) or C.L.S. (cstucky@mcw.edu).

METHODS

TRPM8 gene disruption. The targeting construct deleted 569 base pairs of genomic sequence within exons 13 and 14. Genomic DNA flanking the deleted region (1.9 and 8.7 kb) was PCR-amplified with KOD polymerase (Novagen/Toboyo) from clones 326P3 and 572M11 of the RPCI-22 Bac library (Invitrogen), subcloned and sequenced. Fragments were transferred to pACN, a vector with a neomycin cassette that is removed through self-excision in the male germline³¹. Linearized targeting construct was transfected into E14Tg2A.4 mouse embryonic stem cells (UCSF Core Facility). G418-resistant clones were screened for homologous recombination by PCR and verified by Southern blotting using 5' and 3' flanking probes as well as a neomycin cassette probe. Targeted embryonic stem cell clones were injected into C57/Bl6 blastocysts and chimaeric mice mated to C57/Bl6 females. Heterozygotes were mated to produce paired littermates for all studies. Germline transmission of the mutated allele and excision of the selection cassette were verified by PCR analysis and Southern blotting.

Histology and PCR. Cryostat sections (15 μm thick) were prepared from paraformaldehyde-fixed trigeminal ganglia as described². Sections were incubated overnight at 4 °C with affinity purified guinea pig anti-mouse TRPV1 antiserum diluted 1:1,000 (Julius laboratory), affinity purified rabbit anti-rat TRPM8 antiserum diluted 1:1,000 (kindly provided by M. Tominaga), guinea pig anti-substance P antiserum diluted 1:20,000 (kindly provided by J. Maggio), or goat anti-peripherin antiserum (Santa Cruz Biotechnology). Primary antisera were visualized by subsequent incubation with AlexaFluor 594- or 488-coupled secondary antibody (Invitrogen). For RT-PCR, total RNA was isolated from trigeminal ganglia of TRPM8^{-/-} or TRPM8^{+/+} mice and 1 μg was used to synthesize first-strand complementary DNA using SuperScript II reverse transcriptase (Invitrogen) according to the manufacturer's protocol. PCR was carried out using primer pairs corresponding to nucleotides 1909–1933 and 2907–2931 for mouse TRPM8, and 1681–1710 and 2453–2481 for mouse TRPA1.

Calcium imaging. Dissociation and culturing of mouse trigeminal or dorsal root ganglion neurons and ratiometric calcium imaging were carried out as previously described¹¹. For calcium imaging experiments, analysis was performed on neurons cultured from individual littermates while blind to genotype. Thermal threshold were defined as the temperature at which the response exceeds the standard deviation of the baseline by fivefold.

Skin-nerve preparation and fibre analysis. Mice were anaesthetized with isoflurane and sacrificed via cervical dislocation. Saphenous nerve and skin from the medial dorsum of the hind paw were dissected free and placed corium side up into a tissue bath superfused with oxygen-saturated synthetic interstitial fluid containing (in mM): 123 NaCl, 3.5 KCl, 0.7 MgSO₄, 1.7 NaH₂PO₄, 2.0 CaCl₂, 9.5 sodium gluconate, 5.5 glucose, 7.5 sucrose and 10 HEPES, 290 mOsm, pH 7.45 \pm 0.05, at 32.0 \pm 0.5 °C. The saphenous nerve was desheathed and teased into fine filaments for extracellular recordings as previously described^{16,17}. Single afferent units were identified using an electrical search stimulus in which a Teflon-coated steel needle electrode (2 M Ω impedance, uninsulated tip diameter of 10 μm) was inserted systematically across the skin preparation while square-wave pulses (500 μs , 6 mA) were applied. Following action potential (signal-to-noise ratio > 3) identification, the surrounding tissue was probed to identify the lowest electrical threshold. This point corresponded reliably to the most mechanically sensitive part of the receptive field in mechanically sensitive fibres as determined by calibrated von Frey filaments. Conduction velocity was calculated as previously described¹⁶. Units conducting slower than 1.2 m s⁻¹ were classified as unmyelinated C fibres, those conducting between 1.2 and 10 m s⁻¹ were classified as thinly myelinated A δ fibres, and those exhibiting slowly adapting responses to sustained force were further classified as AM fibres. C fibres and AM fibres were characterized for cold responsiveness. Cold stimuli were delivered as follows: first, physiological zero buffer (32 °C) was applied to the isolated receptive field for 20 s. Next, a cold ramp was applied from 32 to 2 °C over a 20 s duration. Action potentials were recorded and analysed as previously described¹⁶. The number of action potentials evoked during a 32 °C buffer stimulus (20 s) was subtracted from the total number evoked during the cold ramp. For each fibre, the cold threshold was identified as the temperature at which the firing rate exceeded five times the standard deviation of the baseline firing rate sampled during the 32 °C stimulus. All experiments and analyses were performed blind to genotype. One-way ANOVA and Student's *t*-test were used to determine significance between wild-type and mutant responses, as indicated in the figure legends.

Behaviour. All mice (20–35 g) were housed with 12 h light–dark cycle at an ambient temperature of 21 °C and experiments were performed under the policies and recommendations of the International Association for the Study of Pain and approved by the University of California, San Francisco Institution Animal Care and Use Committee. Core body temperature was measured rectally with a

thermocouple probe (Physitemp). A 50% mechanical threshold was determined with von Frey hair filaments using the 'up and down paradigm' starting with 0.1 g and ending with a 2.0 g filament as a cut-off value. Noxious thermal thresholds were determined using an adaptation of the radiant heat test³², and cold/hot plate tests in which the temperature of the platform was varied between +52 to –10 °C. Time to first response for shivering, flinching or hind paw lifting was recorded with a cut-off value of 300 s for cold or 20 s for heat to prevent thermal injury. Responses to evaporative cooling were assessed by applying acetone to the hind paw as previously described¹¹. For the two-plate choice test, animals were placed in a chamber containing identical adjacent platforms with one set to 30 °C and the other adjusted to various temperatures. Mice were free to explore and the total time spent on each surface was recorded over a 5 min period. All data sets were analysed using two- or one-way ANOVA analysis followed by Tukey's HSD post-hoc analysis. All behavioural tests were performed by a single individual who was blind to genotype. Behavioural experiments were performed with F2 generation littermates and thus it is formally possible that strain-polymorphic determinants could contribute to cold preference behaviour if they are closely linked to the TRPM8 locus. Future analysis of animals on a more uniform genetic background will address this issue.

31. Bunting, M., Bernstein, K. E., Greer, J. M., Capecchi, M. R. & Thomas, K. R. Targeting genes for self-excision in the germ line. *Genes Dev.* 13, 1524–1528 (1999).
32. Hargreaves, K., Dubner, R., Brown, F., Flores, C. & Joris, J. A new and sensitive method for measuring thermal nociception in cutaneous hyperalgesia. *Pain* 32, 77–88 (1988).